Available online at www.sciencedirect.com

SciVerse ScienceDirect

Energy Procedia 26 (2012) 31 – 40

Energy Procedia

2nd Trondheim Gas Technology Conference

# A two property catalyst/sorbent pellet design for the sorption-enhanced steam–methane reforming process: Mathematical modeling and numerical analysis

Jannike Solsvik*, Hugo A. Jakobsen

*Department of Chemical Engineering, Norwegian University of Science and Technology (NTNU), N-7491 Trondheim, Norway*

## Abstract

In the present study, the performance of a combined catalyst/sorbent pellet design for the sorption-enhanced steam–methane reforming process has been numerically investigated. The mathematical pellet model formulated for the process describes the evolution of species mole fractions, pressure, total concentration, temperature, mass and heat fluxes, and convection within the voids of the porous pellet. The mass diffusion fluxes are described according to the Maxwell–Stefan and dusty gas models and the effective diffusivities are described employing the parallel pore model. In addition, models proposed in the literature for void fraction changes and product layer diffusion resistance are adopted.

The effectiveness factor is a convenient parameter used in modeling and simulations of chemical reactors indicating the relative importance of diffusion and reaction limitation. In this study, the simulation results presented in terms of effectiveness factors reveal the following noticeable findings for the two pellet diameters analyzed: (i) Knudsen diffusion is significant for the operation conditions set for the simulation study. Hence the pore size distribution within the pellet is significant. (ii) Structural changes within the pellet affects the pellet capacity.



*Keywords:* Multicomponent diffusion, SE-SMR, Mathematical modeling, Pellet simulations, Sorption, $CO_2$ capture

## 1. Introduction

Natural gas is both an important source of energy and an important precursor for chemical materials. The process of sorption-enhanced steam–methane reforming (SE-SMR) is currently an important topic due to its integration of hydrogen production and $CO_2$ separation. Hydrogen has for several decades been an important raw material for the manufacture of commodity chemicals such as ammonia in fertilizer industries and methanol. Increased quantities of $H_2$ are now being used in petroleum refining as sour heavy crude increasingly replaces sweet, light cruds [1]. In the SE-SMR process, $CO_2$ is captured by an integrated sorbent, and the chemical equilibrium is shifted to the product side of the steam–methane reforming (SMR)

*Corresponding author.

*Email addresses:* jannike.solsvik@chemeng.ntnu.no (Jannike Solsvik), hugo.jakobsen@chemeng.ntnu.no (Hugo A. Jakobsen)

1876-6102 © 2012 Published by Elsevier Ltd. Selection and/or peer-review under responsibility of the organizing committee of 2nd Trondheim Gas Technology Conference. Open access under CC BY-NC-ND license.
doi:10.1016/j.egypro.2012.06.007

**Nomenclature**

*Latin Letters*

| | |
|---|---|
| $a$ | parameter |
| $b$ | parameter |
| $c$ | concentration, kmol/m$^3$ |
| $Cp$ | heat capacity, J/(kmol K) |
| $Cp'$ | heat capacity, J/(kg K) |
| $D$ | diffusivity, m$^2$/s |
| $D_{iK}$ | Knudsen diffusivity for species $i$, m$^2$/s |
| $\widetilde{D}_{ij}$ | Maxwell-Stefan diffusivities, m$^2$/s |
| $d$ | diameter, m |
| $h$ | heat transfer coefficient (W/m$^2$/K) |
| $\Delta H$ | heat of reaction, J/kmol |
| $\mathbf{J}$ | molecular diffusion flux, kmol/(s m$^2$) |
| $k_c$ | rate constant, m$^3$/(kmol s) |
| $k$ | mass transfer coefficient (m/s) |
| $N$ | moles per unit volume of sorbent particle, kmol/m$^3$ |
| $M$ | molecular weight, kg/kmol |
| $n$ | number of species in gas mixture |
| $p$ | pressure, Pa |
| $Q$ | heat conductivity flux, J/(m$^2$s) |
| $r$ | radial coordinate, m |
| $r$ | reaction rate, kmol/(kg s) |
| $S$ | molecular source term, kmol/(m$^3$s) |
| $S'$ | heat source term, J/(m$^3$s) |
| $T$ | temperature, K |
| $t$ | time, s |
| $\mathbf{u}$ | molar average velocity, m/s |
| $\mathbf{v}$ | mass average velocity, m/s |
| $x$ | mole fraction |
| $X$ | fractional conversion of CaO to $CaCO_3$ |
| $X^u$ | ultimate conversion of CaO |
| $Z$ | molar volume ratio |

***Greek Letters***

| | |
|---|---|
| $\alpha$ | ratio between volumes of $CO_2$-acceptor and catalyst |
| $\delta$ | average grain diameter, m |
| $\eta$ | effectiveness factor |
| $\epsilon$ | porosity |
| $\lambda$ | conductivity, W/(m K) |
| $\rho$ | density, kg/(m$^3$) |
| $\tau$ | tortuosity |
| $\sigma$ | grain surface area per unit particle volume, 1/m |

***Subscript***

| | |
|---|---|
| cat | catalyst |
| cap | capture, $CO_2$-acceptor |
| eq | equilibrium |
| $i, j, n$ | indicate species type |
| $k$ | reactions (I), (II) or (III) |
| $p$ | pellet |
| pore | pellet pore |
| $PL$ | product layer |
| $r$ | radial direction |
| 1 | void region with the larger pore diameter |
| 2 | void region with the smaller pore diameter |

| ***Superscript*** | |
|---|---|
| *b* | bulk |
| *e* | effective |
| ref | reference state |
| *s* | superficial |
| 0 | initial |

reactions. The reforming reactions (I) and (II), and the water–gas-shift reaction (III) are the most important reactions when converting methane in the presence of steam. When a Ca-based sorbent is integrated in the SMR process, the presumable selective removal of $CO_2$ is represented by reaction (IV). Because the sorbent is effectively consumed in reaction (IV), the SE-SMR process is dynamic in nature. However, a sorbent regeneration step (V) is necessary to make the SE-SMR process economically viable.

$$CH_4 + H_2O = CO + 3\,H_2 \quad \text{(I)}$$

$$CH_4 + 2\,H_2O = CO_2 + 4\,H_2 \quad \text{(II)}$$

$$CO + H_2O = CO_2 + H_2 \quad \text{(III)}$$

$$CO_2 + CaO = CaCO_3 \quad \text{(IV)}$$

$$CaCO_3 = CO_2 + CaO \quad \text{(V)}$$

The SE-SMR process can be operated using either of two different pellet designs: the two-pellet design or the one-pellet design. In the two-pellet design, the $CO_2$ capture property and the reformer catalytic property are separated into two different pellets. On the other hand, the one-pellet design unifies the catalytic and capture properties in a single pellet type.

In the present study the simulation results are presented in terms of an effectiveness factor which is a convenient parameter frequently used in reactor design. The effectiveness factor for solid–gas reactions is defined as [2]:

$$\eta = \frac{\text{actual overall rate of reaction}}{\text{rate of reaction with surface conditions}} \quad (1)$$

Thus the effectiveness factor of the sorption and catalytic reactions will indicate diffusional limitations within the porous structure of the pellet. For a strongly diffusion limited process $\eta << 1$, and for a reaction limited process $\eta \rightarrow 1$. For a pellet holding both the reformer catalytic property and the $CO_2$ capture property, the effectiveness factor may exceed the unit value for the capture reaction because, due to the reformer reactions, a higher $CO_2$ partial pressure may temporarily exists within the pellet than present at the pellet surface.

For a chemical reaction such as the CaO carbonation reaction (IV), the definition of the effectiveness factor cannot be used in its current form, because equation (1) becomes ill-conditioned for the capture reaction (IV) when the surface is fully saturated with $CO_2$. To overcome this problem, an alternative definition is required for the capture reaction. Thus, in this study, the following definition of the effectiveness factor is proposed for the $CO_2$ capture reaction (IV):

$$\eta_{\text{cap}} = \frac{\text{actual overall rate of reaction}}{\text{reference rate of reaction, } r_{\text{ref}}} \quad (2)$$

Structural changes within the sorbent particle is a drawback in the SE-SMR process, i.e. the sorbent may lose its $CO_2$-capture capacity due to product layer formation and sintering. Attempts have been made on modeling structural changes within sorbents for $CO_2$ capture; e.g. Stendardo and Foscolo [3] describes a mathematical model of a particle made up of very small spherical grains which grow during the gas–solid reaction due to solid product formation around the grains, thus the particle void fraction is reduced as the reaction proceeds. The structural changes in the spherical grains are taken into account in the proposed model by the inclusion of a variable diffusion coefficient of the gaseous reactant through the developing product layer.

Recently Solsvik and Jakobsen [4] performed a numerical study of a two property catalyst/sorbent pellet design for the SE-SMR process focusing on modeling complexity and parameter sensitivity analysis. In the present study, the work of Solsvik and Jakobsen [4] is further extended to elucidate the effects of product layer diffusion, void fraction changes and Knudsen diffusion for smaller pellet diameters, i.e. 0.5 (fluidized bed) and 3 mm versus 7 mm (fixed bed).

## 2. Mathematical model

In the sequent the combined catalyst/sorbent model is outlined. Further details on the model and numerical solution algorithm using the orthogonal collocation method are given by Solsvik and Jakobsen [4]. The reactor operating conditions used are given in table 2.

The continuity equation, species mole balances and heat balance are given by, respectively [4, 5, 6, 7]:

$$\epsilon_p \frac{\partial c}{\partial t} + \frac{1}{r^2}\frac{\partial}{\partial r}(r^2\, u_r^s\, c) = \sum_i S_i \tag{3}$$

$$\epsilon_p \frac{\partial}{\partial t}(c\, x_i) + \frac{1}{r^2}\frac{\partial}{\partial r}(r^2\, u_r^s\, c\, x_i) = -\frac{1}{r^2}\frac{\partial}{\partial r}(r^2\, J_{i,r}) + S_i \tag{4}$$

$$\left((1-\epsilon_p)Cp'_p\rho_p + \epsilon_p c\sum_{i=1}^{n} x_i\, Cp_i\right)\frac{\partial T}{\partial t} = -c\sum_{i=1}^{n} x_i\, Cp_i\, v_r^s\,\frac{\partial T}{\partial r} - \frac{1}{r^2}\frac{\partial}{\partial r}(r^2 Q_r) + S' \tag{5}$$

where the mass source term and the heat source term [8] are given by correlations (6) and (7):

$$S_i = \frac{1-\epsilon_p}{1+\alpha}\rho_{cat} r_i + \frac{1-\epsilon_p}{1+\frac{1}{\alpha}}\rho_{cap} r_{cap,i} \tag{6}$$

$$S' = \frac{1-\epsilon_p}{1+\alpha}\rho_{cat}\sum(-\Delta H_{r_k})r_k + \frac{1-\epsilon_p}{1+\frac{1}{\alpha}}\rho_{cap} r_{cap,j}(-\Delta H_{r_{cap,j}}) \tag{7}$$

Table 1 holds the initial and boundary conditions applied in the simulations.

The Darcy law (14) is adopted which expresses the relationship between the viscous flow velocity and the pressure drop within the pellet [9, 10].

$$\mathbf{v} = -\frac{d_{\text{pore}}^2}{32\mu}\nabla p \tag{14}$$

The random pore model [11] for bi-disperse pore system suggest the effective diffusivity (15) where $\epsilon_1$ and $\epsilon_2$, in this work, denote the inter-agglomerate and inter-grain voids, respectively. Thus, the void within the pellet is divided into two different regions in which each region constitute a void fraction characterized by cylindrical pores having a mean pore radius, $r_{\text{pore},1}$ (inter-agglomerate void) and $r_{\text{pore},2}$ (inter-grain void).

$$D^e = D_1\epsilon_1^2 + \frac{\epsilon_2^2(1+3\epsilon_1)}{1-\epsilon_1}D_2 \tag{15}$$

The Knudsen diffusion coefficient is computed as [12]:

$$D_{i,K} = 97.0\frac{d_{\text{pore}}}{2}\left(\frac{T}{M_i}\right)^{1/2} \tag{16}$$

whereas the binary diffusion coefficients are given by [13]:

$$D_{i,j} = \frac{0.00266\cdot 101325\, T^{3/2}}{0.01^2\, p\,\Omega_{ij}\Sigma_{ij}^2 M_{ij}^{1/2}} \tag{17}$$

Table 1. Initial and boundary conditions.

Initial conditions:

$$\left.\begin{aligned} x_i &= x_i^b \\ J_{i,r} &= 0 \\ T &= T^b \\ Q_r &= 0 \\ c &= c^b \end{aligned}\right\} \quad \text{for} \quad t = 0,\ \forall\, r \tag{8}$$

Boundary conditions for symmetry point, $r = 0$:

$$J_{i,r} = 0 \tag{9}$$

$$Q_r = 0 \tag{10}$$

Boundary conditions for surface, $r = r_p$:

$$-k_i\,(c_i^b - x_i\,c) = J_{i,r} + u_r^s\,c\,x_i \tag{11}$$

$$Q_r + c\,Cp_g\,T\,v_r = -h(T^b - T) \tag{12}$$

$$c = c^b \tag{13}$$

The molecular mass diffusion fluxes [6] are described according to the Maxwell–Stefan (18) [14, 15] and dusty gas (19) [16, 17] models:

$$\mathbf{J}_i = \frac{-c\nabla x_i + \sum\limits_{\substack{j=1 \\ j\neq i}}^{n} \frac{\mathbf{J}_j x_i}{\widetilde{D}_{ij}}}{\sum\limits_{\substack{j=1 \\ j\neq i}}^{n} \frac{x_j}{\widetilde{D}_{ij}}} \tag{18}$$

$$\mathbf{J}_i = \frac{\sum\limits_{\substack{j=1 \\ j\neq i}}^{n} \frac{\mathbf{J}_j x_i}{\widetilde{D}_{ij}} - \frac{c_i \mathbf{v}^*}{D_{iK}} - c\nabla x_i}{\sum\limits_{\substack{j=1 \\ j\neq i}}^{n} \frac{x_j}{\widetilde{D}_{ij}} + \frac{1}{D_{iK}}} \tag{19}$$

The reaction kinetic model of the reforming and shift reactions by Xu and Froment [18], and the $CO_2$ capture for $CaO/Ca_{12}Al_{14}O_{33}$ (75/25 wt%) sorbents by Li and Cai [19] were adopted in this study. The fractional conversion rate of CaO to $CaCO_3$ is given by [19]:

$$\frac{\mathrm{d}X}{\mathrm{d}t} = k_c \left(1 - \frac{X}{X^u}\right)^{2/3} (C_{CO_2} - C_{eq,CO_2})^{(\frac{p}{p_0})^{0.083}} \tag{20}$$

During the reaction process CaO reacts with $CO_2$ and converts into $CaCO_3$ and reduce the void fraction within the pellet. The correlation between the reduction in void fraction and the CaO conversion suggested by Stendardo and Foscolo [3] is on the form:

$$\partial\epsilon = -C \cdot \partial X \tag{21}$$

A progressively increasing transport resistance develops in the pellet as a consequence of $CaCO_3$ formation. The product layer diffusivity correlation used in this study is based on the closure proposed by Stendardo

Table 2. Specifications of the reactor operating conditions used in the simulations of the SE-SMR process.

| | | |
|---|---|---|
| $d_p$ (mm) | 0.5 and 3 | |
| $d_{\text{pore},1}$ (nm) | 50 | |
| $d_{\text{pore},2}$ (nm) | 2 | |
| $\epsilon_p^0$ (-) | 0.50 | |
| $\tau_p$ (-) | 3.5 | |
| $p^b$ (bar) | 15 | |
| $T^b$ (K) | 800 | |
| $u^b$ (m/s) | 1.89 | |
| $\rho_{\text{cat}}$ (kg/m$^3$) | 2300 | |
| $\rho_{\text{cap}}$ (kg/m$^3$) | 2500 | |
| $k_{\text{cat}}$ (W/m K) | 25 | |
| $Cp_{\text{cat}}$ (J/kg K) | 1000 | |
| $\alpha$ (-) | 4 | |
| $r_{\text{ref}}$ (kmol/kg s) | 0.045 | |
| $x_i^b$ (-) | Case A | Case B |
| $CH_4$ | 0.212 | 0.183 |
| CO | $6.358 \cdot 10^{-5}$ | $5.56 \cdot 10^{-4}$ |
| $CO_2$ | 0.008 | $2.0 \cdot 10^{-4}$ |
| $H_2$ | 0.026 | 0.076 |
| $H_2O$ | 0.713 | 0.698 |
| $N_2$ | 0.041 | 0.042 |

and Foscolo [3]:

$$D_{\text{PL}} = D_{0,\text{PL}} \exp\left( - a \left[ \frac{X}{X^u} \right]^b \right) \tag{22}$$

The reaction rate (20) is modified in accordance to the work of Stendardo and Foscolo [3] including the effect of the product layer diffusion resistance by the variable diffusion coefficient (22) of the gaseous reactant through the developing product layer:

$$\frac{\partial X}{\partial t} = \frac{k_c (1 - \frac{X}{X^u})^{2/3} (C_{\text{CO}_2} - C_{\text{eq,CO}_2})^{(p/p_0)^{0.083}}}{1 + \frac{N_{\text{Ca}} k_c}{2 D_{\text{PL}} \sigma_{0,\text{CaO}}} \delta_{\text{CaO}} \sqrt[3]{1 - X} \left( 1 - \sqrt[3]{\frac{1-X}{1-X+XZ}} \right)} \tag{23}$$

## 3. Results and Discussion

In the present study a combined catalyst/sorbent pellet design for the SE-SMR process has been numerically investigated. The mathematical modeling and sensitivity study focus on the effects of: (i) product layer resistance and void fraction reduction due to the reaction of $CO_2$ with the sorbent, (ii) pore size distribution within the pellet, (iii) pellet diameter and intra-particle diffusion resistance, and (iv) bulk phase species composition. The simulation results are presented in terms of the effectiveness factor (1) for the reformer reactions (I) and (II), whereas the effectiveness factor (2) is adopted to describe the intra-particle process of $CO_2$ reaction with the sorbent (IV).

The porous structure of the pellet assumes to result from compressed powder composed of agglomerates which have either catalytic (reforming reactions) or $CO_2$ capture properties. The agglomerates can be further divided into grain units, hence, the voids within the porous pellet body arise from inter-grain pores and inter-agglomerate channels [4]. The sensitivity to pore size distribution adopting the random pore model (15) is given in figure 1. For the simulation conditions applied in this study, the effect of Knudsen diffusion due to the pore size distribution has a significant effect on the computed effectiveness factors. Due to the significant Knudsen diffusion contribution, the simulation results of the dusty gas model deviates from the results obtained with the Maxwell–Stefan model.

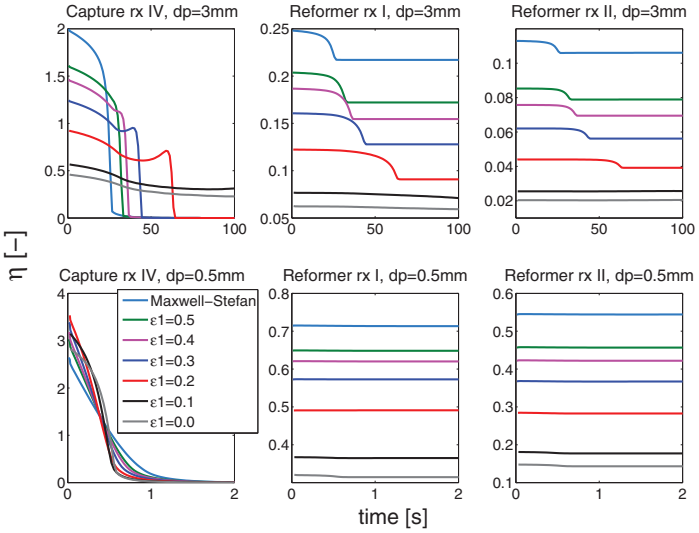


(a) Bulk gas composition: case A in table 2

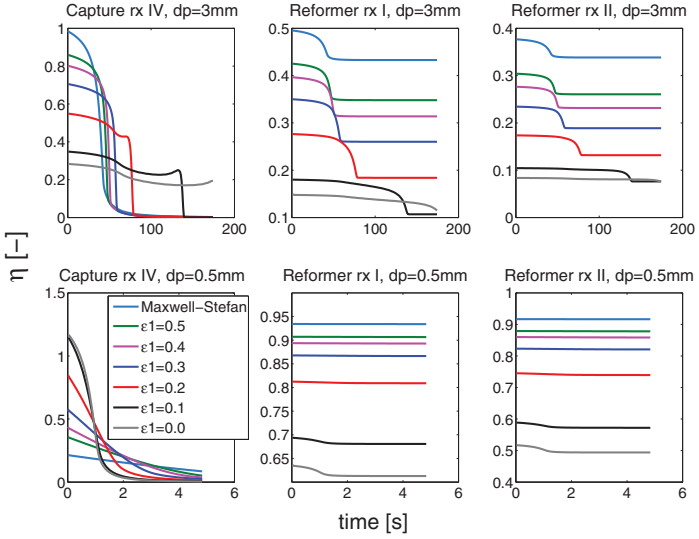


(b) Bulk gas composition: case B in table 2

Fig. 1. Sensitivity to pore size distribution using the dusty gas model. The results of the combined bulk and Knudsen diffusion model (dusty gas) are compared with the pore size independent Maxwell–Stefan (bulk diffusion) model. Considering equation (15), $\epsilon_1 + \epsilon_2 = \epsilon_p = 0.5$ where $r_{\text{pore},1} = 25\text{nm}$ and $r_{\text{pore},2} = 1\text{nm}$ characterize the mean pore radius of the void regions $\epsilon_1$ and $\epsilon_2$, respectively. Product layer is not considered.

In the SE-SMR process a product layer limits the capture capacity. Based on the work of Stendardo and Foscolo [3], the effect of the product layer resistance is modeled by use of a product layer diffusivity. A natural sorbent was used in the work of Stendardo and Foscolo [3], thus to employ the effective reaction rate model suggested by these authors, the model has been modified to fit the kinetics of the synthetic sorbent applied in the present study. However, the product layer diffusivity model suggested for the natural sorbent is adopted in this work without any modifications due to the current lack of experimental data for the synthetic sorbent. It is assumed that the parameter values for natural and synthetic sorbents is similar and a sensitivity study is performed for the presumably most critical parameters, i.e. $a$ and $b$ in equation (22). The simulation

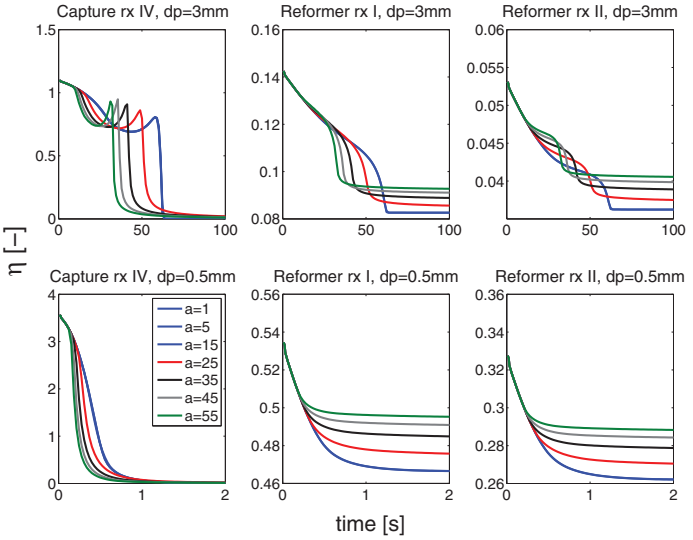


(a) Bulk gas composition: case A in table 2

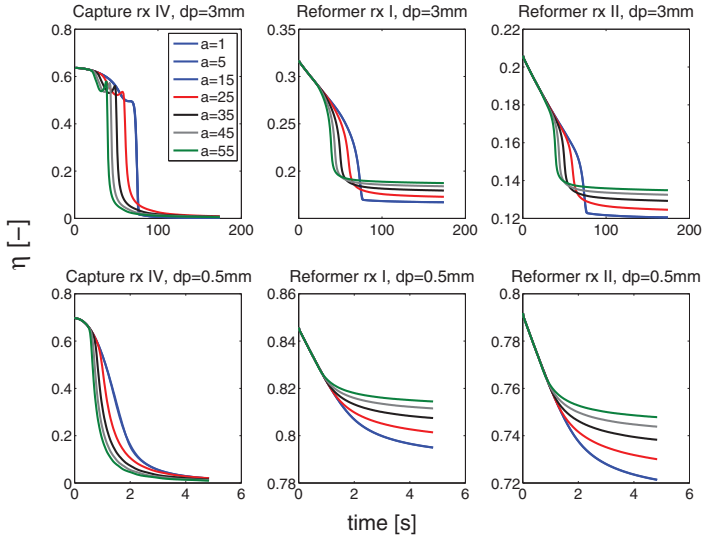


(b) Bulk gas composition: case B in table 2

Fig. 2. Product layer diffusion resistance. Sensitivity to parameter $a$ in equation (22). The simulations are performed with the dusty gas model with pore size distribution $\epsilon_1 = 0.25$ and $\epsilon_2 = 0.25$ in equation (15).

results are presented i figures 2 and 3.

The modeling work on product layer is complex and far from complete. Mess et al.[20] studied $CO_2$ diffusion through $CaCO_3$ product layer on CaO. The authors found that the carbonation rate decreased more rapidly with time than would be expected from diffusion through a uniform product layer. Dennis and Pacciani [21] claimed that it is not possible to model the diffusion of $CO_2$ through the product layer by only determine a value of the diffusivity of $CO_2$ passing through the growing layer of product. The authors claimed that the model must also take into account the disruption of the product layer. However, the stress needed to disrupt the product layer may be significantly affected by gross changes in the morphology of the layer due to sintering in some circumstances.

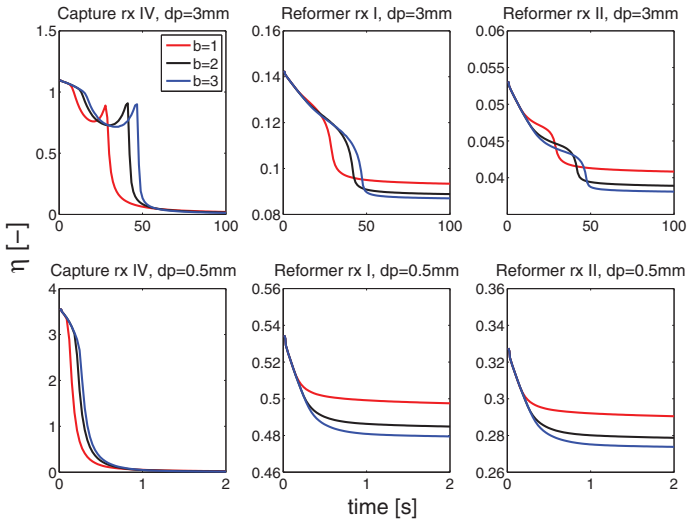


(a) Bulk gas composition: case A in table 2

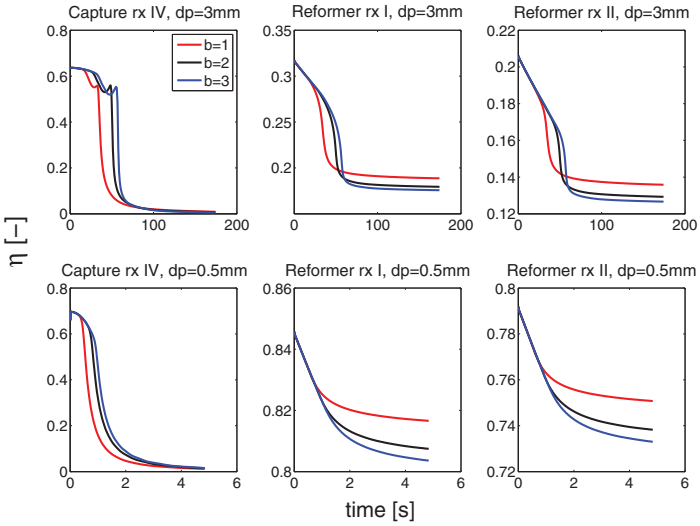


(b) Bulk gas composition: case B in table 2

Fig. 3. Product layer diffusion resistance. Sensitivity to parameter $b$ in equation (22). The simulations are performed with the dusty gas model with pore size distribution $\epsilon_1 = 0.25$ and $\epsilon_2 = 0.25$ in equation (15).

The SE-SMR process is dynamic in nature and hence the effectiveness factors change with the fractional conversion of the solid sorbent; figures 1–3. In addition, both the pellet size and bulk gas phase composition effect the process. The smaller pellet diameter reaches its ultimate $CO_2$ capture capacity within a few seconds, whereas it may take over 30 seconds for the larger pellet. The studied effects at the pellet level should be further evaluated to elucidate the impacts at the reactor level.

For the capture reaction (IV), some simulation cases gave effectiveness factor values that exceeded the unit value because of the combined catalyst/sorbent properties within the pellet. Thus, due to the reformer reactions, a higher $CO_2$ partial pressure temporarily existed within the pellet that present at the pellet surface. The conventional two-pellet design (catalyst and sorbent properties separated in different pellets) is put in disfavor considering the possible high effectiveness factor values achievable with the combined catalyst/sorbent design.

## 4. Concluding Remarks

A numerical investigation of a combined catalyst/sorbent pellet design for the SE-SMR process has been performed in the present study. Structural changes due to the reaction between $CO_2$ and the solid sorbent are modeled by inclusion of a variable product layer diffusion coefficient of the gaseous $CO_2$ through the developing solid layer; and moreover, a correlation for the void fraction reduction with the sorbent conversion is adopted. Furthermore, influence of Knudsen diffusion due to pore size distribution is analyzed adopting a random pore model to describe the effective diffusivities of the dusty gas model. Intra-particle diffusional limitations are influenced by the pellet size, hence, in this study, pellet diameters of 0.5 mm and 3 mm are adopted in the simulations. Simulations are performed with two cases of bulk gas phase compositions due to the effects on the chemical kinetics of the reformer and $CO_2$ capture reactions.

Modeling of both the pore size distribution and structural changes within the pellet are important for improved model prediction of the SE-SMR process. Hence, the pore size distribution within the pellet is an important model parameter that should be determined; and moreover, correlations describing the void fraction decrease with the sorbent fractional conversion and transport resistance due to product layer growth should be developed for the pellet design adopted in the present study because the correlations found in the literature are not based on this particular pellet design.

Simulations on the reactor level are required to elucidate the effects of pore size distribution and structural changers on the reactor performance. Moreover, in order to perform reactor simulations with a homogeneous model, the effectiveness factor (2) is not sufficient.

## References

[1] D. P. Harrison, Sorption-enhanced hydrogen production: A review, Ind. Eng. Chem. Res. 47 (2008) 6486–6501.
[2] H. S. Fogler, Elements of chemical reaction engineering, Prentice Hall, 2006.
[3] S. Stendardo, P. U. Foscolo, Carbon dioxide capture with dolomite: A model for gas–solid reaction within the grains of a particulate sorbent, Chemical Engineering Science 64 (2009) 2343–2352.
[4] J. Solsvik, H. A. Jakobsen, A numerical study of a two property catalyst/sorbent pellet design for the sorption-enhanced steam–methane reforming process: Modeling complexity and parameter sensitivity study, Chemical Engineering Journal 178 (2011) 407–422.
[5] K. R. Rout, J. Solsvik, A. K. Nayak, H. A. Jakobsen, A numerical study of multicomponent mass diffusion and convection in porous pellets for the sorption-enhanced steam methane reforming and desorption processes, Chemical Engineering Science 66 (2011) 4111–4126.
[6] J. Solsvik, H. A. Jakobsen, Modeling of multicomponent mass diffusion in porous spherical pellets: Application to steam methane reforming and methanol synthesis, Chemical Engineering Science 66 (2011) 1986–2000.
[7] K. R. Rout, H. A. Jakobsen, Reactor performance optimization by the use of a novel combined pellet reflecting both catalyst and adsorbent properties, Fuel Processing Technology 99 (2012) 13–34.
[8] H. K. Rusten, E. Ochoa-Ferndez, H. Lindborg, D. Chen, H. A. Jakobsen, Hydrogen Production by Sorption-Enhanced Steam Methane Reforming Using Lithium Oxides as $CO_2$-Acceptor, Ind. Eng. Chem. Res. 46 (2007) 8729–8737.
[9] H. A. Jakobsen, Chemical reactor modeling. Multiphase reactive flows, Springer, 2008.
[10] R. Krishna, Problems and pitfalls in the use of the Fick formulation for intraparticle diffusion, Chemical Engineering Science 48 (5) (1993) 845–961.
[11] J. M. Smith, Chemical engineering kinetics, McGraw-Hill, 3 edn., 1981.
[12] C. J. Geankoplis, Transport processes and separation process principles, Prentice Hall, 2003.
[13] R. C. Reid, J. M. Prausnitz, B. E. Poling, The properties of gases and liquids, McGraw-Hill Book Company, 1987.
[14] J. C. Maxwell, On the dynamical theory of gases, Phil. Trans R. Soc. 157 (1866) 49–88.
[15] J. Stefan, Über das Gleichgewicht und die Bewegung insbesondere die Diffusion von Gasgemengen, Sitzber. Akad. Wiss. Wien 63 (1871) 63–124.
[16] R. Jackson, Transport in porous catalysts, Elsevier, 1977.
[17] E. A. Mason, A. P. Malinauskas, Gas Transport in Porous Media: The Dusty Gas Model, Elsevier, 1983.
[18] J. Xu, G. F. Froment, Methane steam reforming, methanation and water-gas shift: I. Intrinsic kinetics, AIChE Journal 35 (1989) 88–96.
[19] Z.-S. Li, N.-s. Cai, Modeling of multiple cycles for sorption-enhanced steam methane reforming and sorbent regeneration in fixed bed reactor, Energy & Fuels 21 (2007) 2909–2918.
[20] D. Mess, A. F. Sarofim, J. P. Longwell, Product layer diffusion during the reaction of calcium oxide with carbon dioxide, Energy and Fuels 13 (1999) 999–1005.
[21] J. S. Dennis, R. Pacciani, The rate and extent of uptake of $CO_2$ by a synthetic, CaO-containing sorbent, Chemical Engineering Science 64 (2009) 2147–2157.